PHILOSOPHICAL TRANSACTIONS OF THE ROYAL SOCIETY A MATHEMATICAL, PHYSICAL & ENGINEERING SCIENCES

Additional Heating Experiments on JET with Ion-Cyclotron Waves

J. Jacquinot, V. Bhatnagar, H. Brinkschulte, M. Bures, S. Corti, G. A. Cottrell, M. Evrard, D. Gambier, A. Kaye, P. P. Lallia, F. Sand, C. Schueller, A. Tanga, K. Thomsen and T. Wade

Phil. Trans. R. Soc. Lond. A 1987 **322**, 95-107
doi: 10.1098/rsta.1987.0040

Phil. Trans. R. Soc. Lond. A **322**, 95–107 (1987)
Printed in Great Britain

Additional heating experiments on JET with ion-cyclotron waves

By J. Jacquinot, V. Bhatnagar, H. Brinkschulte, M. Bures, S. Corti, G. A. Cottrell, M. Evrard, D. Gambier, A. Kaye, P. P. Lallia, F. Sand, C. Schueller, A. Tanga, K. Thomsen and T. Wade

*JET Joint Undertaking, Abingdon, Oxfordshire, OX*14 3*EA, U.K.*

The physics aspects of tokamak plasma heating with ion-cyclotron waves are reviewed in the light of initial experiments in JET. The power coupled to the plasma has reached 5.5 MW. Central temperatures of both the ions and electrons have more than doubled. Peak values reached 5 keV. The data are well represented by a law $(\Delta T_{e0}+\Delta T_{i0}) = aP_{RF}/\langle n_e\rangle$ with $a = (1.5\text{–}2)\times 10^{13}$ keV W^{-1} m^{-3}.

The power deposition appears highly localized in the vicinity of the cyclotron resonance and preliminary experiments on the effect of local deposition on confinement have been performed. The best heating conditions are obtained with central power deposition or with a slightly outboard shift for best ion heating. These optimum conditions also correspond to large sawtooth relaxation of the temperature of the plasma core.

1. Introduction and physics background

The large electrical current circulating in the plasma of a tokamak configuration serves two distinct functions:

(*a*) it provides the poloidal magnetic field, which combined with the externally induced toroidal field provides the basic confining topology;

(*b*) it provides a heating source resulting from the finite plasma resistivity; in JET, the ohmic heating power is typically between 2 and 3 MW.

As the plasma temperature rises, the collisions between electrons become rarer and the electrical resistivity decreases. The overall result is a decrease of the ohmic power following a $T_e^{-\frac{3}{2}}$ law (T_e is the plasma electron temperature). Therefore the attainment of higher temperatures require other means of plasma heating.

The research on the physics of confinement also requires additional heating systems to break the link between confinement and heating that always prevails in experiments with ohmic heating only.

Additional heating programmes on tokamak plasmas started 15 years ago when the injection of hydrogenic atom beams was the only method available with power capability comparable with the ohmic power input. These early experiments (Équipe TFR 1977) were done at modest power (650 kW) with limited pulse length (100 ms). These experiments already showed significant ion heating but revealed basic difficulties in increasing the electron temperature. Duesing (this symposium) describes such a neutral-beam system on JET and shows the considerable progress made in the past ten years.

The JET additional heating programme of extension to full performance is based on two different plasma heating methods:

neutral-beam injection (NBI) with a total of 10 MW, in two units, of 'high-grade power',

and

ion-cyclotron range of frequency (ICRF) with a total of 16 MW, in eight units, of 'high-grade power',

where for both 'high-grade power' refers to the power deposited in the plasma centre, defined as 25% of the plasma volume. For ICRF, it is estimated that this specification would require 32 MW at the output of the RF generator plant.

The physics of NBI heating is solidly documented and well proven by experiments where it is normally the major heating method. However, at the high injection energies required for penetration of large plasmas the neutralization efficiency decreases strongly with serious consequences on the technological complexity and cost of the system. Despite this complexity, good progress has been achieved, a first NBI unit has been completed and the first NBI experiments that have just started on JET are discussed by Duesing (this symposium). On the contrary, the efficiency of ICRF does not, in theory, appear to be penalized by the increased plasma size.

Additional heating by using propagation and damping of electromagnetic waves in the plasma has been contemplated for a long time (Hooke *et al.* 1962; Pease *et al.* 1966; Adam & Samain 1971). Its main practical motivation is an overall power transfer efficiency that is potentially much higher than in the neutral beam injection system. However, the complexity of the physical processes involved in the method appeared much greater than expected and triggered a broad research on basic plasma wave interactions in an extremely wide spectrum of frequency: 10–100 GHz. It was only recently that self-consistent heating schemes could be put forward. These are based on fundamental plasma resonances:

the ion-cyclotron resonance (ICRH);

the electron-cyclotron resonance (ECRH);

the electron–ion hybrid resonance or lower hybrid resonance (LHRH).

The maximum value of the main toroidal field on the magnetic axis of JET being 3.4 T, the cyclotron frequencies on axis are 51 MHz for protons and 95 GHz for electrons at rest. The lower hybrid frequency occurs at an intermediate frequency, 2–5 GHz, depending on the electron density. The subject has stimulated the interest in procuring high-power sources (table 1) by using advanced technology in the field of tetrodes, klystrons and gyrotrons. All three types of heating systems are operated on tokamaks in the world's fusion programme. JET has chosen ICRH as being for the moment, the best combination in the availability of high-power sources and in the understanding of the basic wave plasma phenomena. This method appears complementary to the neutral-beam system: when used separately, a larger domain of plasma operation can be explored; when used simultaneously, synergistic effects on wave damping and current drive may be expected.

TABLE 1

main RF-heating methods	high-power device	unit power available for JET conditions (20 s pulses)
cyclotron resonance with a minority species, H or ^{3}He	tetrode	2 MW broad band (20–100 MHz)
electron-cyclotron resonance	gyrotron	250 kW at 70 GHz
hybrid resonance between plasma electrons and ions	klystron	500 kW at 3.7 GHz 250 kW at 4.6 GHz

On the technical side, the JET ICRF system (Kaye *et al.* 1985) will deliver, when completed, 32 MW in eight antennas and will be operated in pulses lasting 20 s. Each unit can be operated at any particular frequency between 23 and 57 MHz. Groups of units will also be operated at the same frequency and phase-locked. Compared with the previous generation of experiments, this implies a formidable increase in the size of the system: in particular, the amount of energy delivered to the plasma will be increased by more than two orders of magnitude.

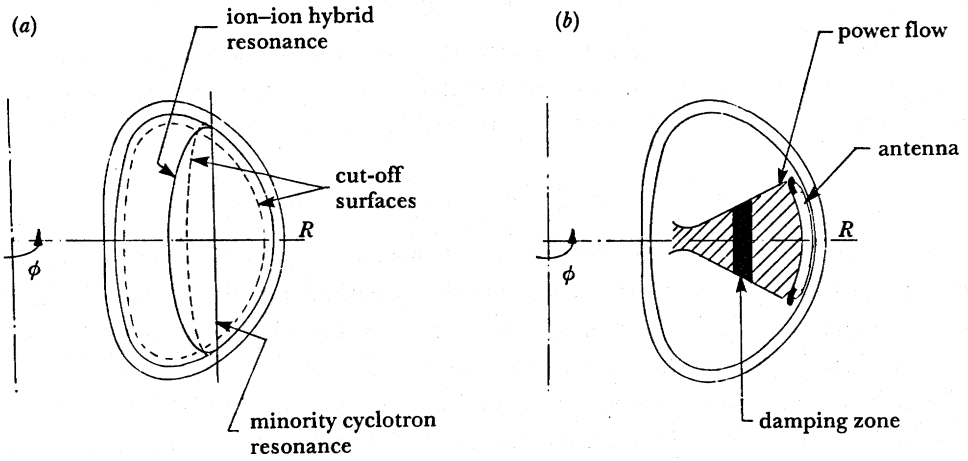

FIGURE 1. Diagram of the geometrical features of the ion-cyclotron wave propagation and damping. (*a*) Singular surfaces of the fast magnetosonic wave in a tokamak. The position of the cyclotron resonance can be varied by selection of the wave frequency. (*b*) The power flow emitted by the antenna stays within the envelope shown and is transferred to minority ions in the vicinity of the cyclotron resonance.

The major physics aspects of ICRF heating are illustrated on figure 1. Figure 1*a* represents the singular layers (according to the cold-plasma description) of the wave launched by the antenna as it penetrates in the tokamak with a constant value of $k_\parallel R$, an invariant resulting from the toroidal symmetry ($k_\parallel$ is toroidal wavenumber; R is major radial position).

The outer cutoff layer corresponds to the decrease of the electron density below the value necessary for propagation of the fast wave. The wave radiated by the antenna has to tunnel through this evanescent region.

The cyclotron resonance is given by

$$\omega_c = ZeB_0 R_0/Rm, \tag{1}$$

where the index 0 indicates the value of the magnetic field B and the radial position R on the magnetic axis. Z is the atomic charge of the ion species. Note that a fusion plasma normally contains several ion species mainly deuterium and tritium but also hydrogen and helium. In JET, for reasons of optimum damping, the resonance is normally adjusted to occur in the plasma centre for a small minority (5–10%) of protons or helium-3 ions.

Equation 1 expresses the R^{-1} dependence of the magnetic field in a toroidal device. This property allows to adjust the resonance at any radial position by simple variation of the ratio B/ω. Throughout the text we call R_r the position of this resonance.

Further inboard, we find a cutoff resonance pair arising from the occurrence of a hybrid resonance between the majority ion species (deuterium now and later a deuterium–tritium

mixture) and the minority-ion species. This hybrid resonance is normally very close to majority cyclotron resonance. More precisely, the position of the central cutoff is separated from the cyclotron resonance by (considering a hydrogen minority in a deuterium plasma):

$$\Delta R_{rc} \approx -\tfrac{1}{2}\eta R_r \tag{2}$$

and the width of the evanescent zone between the cutoff and the hybrid resonance is:

$$\Delta R_e \approx -\tfrac{1}{4}\eta R_r. \tag{3}$$

In the expressions $\eta = n_H/n_D$ represents the density ratio of the two ion species.

These cutoff and resonance layers are sharply defined only in the cold plasma approximation. In a hot plasma, the power absorbed near the cyclotron resonance per unit volume is given by

$$P_i = \tfrac{1}{4}\sqrt{\pi}\epsilon_0\,\omega_{pi}^2\,(E_+^2/k_\parallel V_i)\,\exp-[(\omega-\omega_{ci})/k_\parallel V_i]^2,$$

an expression that underlines the importance of the Doppler-width term $(\omega-\omega_{ci})/k_\parallel V_i$, and of the electric field component E_+ that rotates in the direction of the ion motion ($k_\parallel$, wavenumber parallel to magnetic field; V_i, thermal-ion velocity; ω_{pi}, ion plasma frequency).

The value of E_+ is strongly affected by the resonance. For fundamental cyclotron resonance in a high density plasma the excessive number of resonant ions strongly shield the E_+ component of the RF field (analogous to the familiar skin effect). This leads to weak wave damping. This problem is solved by choosing a resonance with a minority-ion species, with a relative concentration typically 5–10%. The shielding effect is much reduced as the number of resonating ions is smaller. Furthermore, a hybrid resonance between the minority and the bulk ions is generated and greatly restores a large value of E_+. With this minority heating technique a very efficient damping zone is set in the plasma centre and in most condition of interest, the wave is absorbed during a single pass across the plasma.

Single-pass absorption simplifies the determination of the wave power flow as it allows the

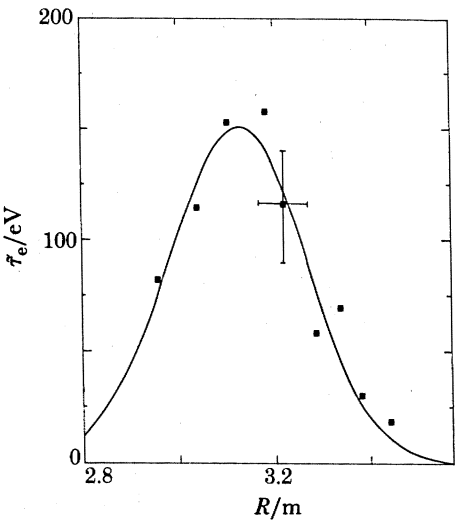

FIGURE 2. Amplitude of the electron temperature modulation resulting from power modulation against radial position. Such experiments can determine the localization of energy deposition. Modulation 1.25 MW peak to peak, 5 Hz, He^3 minority, $I_p = 3$ MA, $B_\phi = 3.4$ T. The magnetic axis is at 3.1 m and the plasma radial extension is 2.2 m.

use of ray-tracing techniques (Bhatnagar *et al.* 1983). As the group velocity vector is nearly parallel to the density gradient, the power flow focuses near the plasma centre as illustrated in figure 1*b*. The deposition of the power can therefore be highly localized with ICRF if the antenna is located near the equatorial plane. In JET, the power is deposited with a half-width of 30 cm in the radial direction. These results are confirmed by sophisticated full-wave solutions (Hellsten *et al.* 1985; Itoh *et al.* 1986) and by experimental measurements with various techniques. For instance, modulation experiments show a very localized response of the electron temperature (figure 2) in agreement with expectations.

Cyclotron damping transfers the wave energy into perpendicular energy of the resonating minority ions that become much hotter than the background plasma and develop a non-Maxwellian distribution function (see figure 3). Finally, collisions transfer the energy of the minority to the main plasma species.

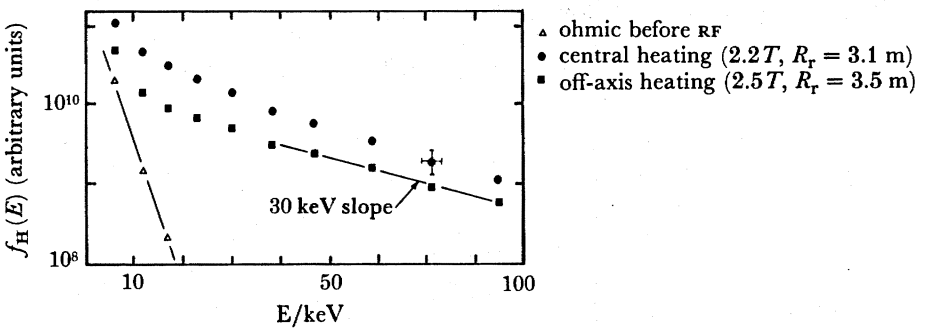

FIGURE 3. Energy distribution function of the hydrogen minority measured by charge-exchange spectrometry in the plasma centre showing the high-energy tail and the non-Maxwellian distribution resulting from minority heating; $P_{RF} = 3$ MW.

2. MAIN RESULTS

The first ICRF experiments on JET started in 1985. By the end of the year 6 MW were coupled to the plasma by 3 antennas, each connected to a tandem amplifier of 3 MW output. The description of the apparatus as well as the initial results of plasma heating have already been reported (Jacquinot *et al.* 1985, 1986). The most recent results were reported in detail by several of us at the conference of the European Physical Society at Schliersee in April 1986. In the present paper, the main aspects of ICRF heating, as revealed after just one year of experimentation, are summarized. The impurity release and radiation effects due to RF heating and the description of the measurement techniques have been left out and treated separately by Engelhardt and Stott (this symposium).

2.1. *Experimental conditions, overview of heating effects*

Both hydrogen and helium-3 minority heating experiments have been performed in deuterium. The typical plasma conditions are summarized in table 2. In this table, the frequency and the magnetic field correspond to power deposition near the plasma centre. The plasma density values correspond to the extreme operating range set, on the upper end, by the disruptive limit and on the lower end by recycling and gas desorption from the wall and the limiters.

Figures 3–6 illustrate the heating effects in the hydrogen minority case (first column of table 2 with $n_e = 2.4\ 10^{19}$). This particular case corresponds to the maximum ratio of RF power to ohmic power which could be achieved.

Figure 4 gives the evolution of the central deuterium and electron temperature when 5.2 MW is coupled to the plasma. The time average temperature roughly doubles from the initial ohmic level. Periodic fluctuations are clearly visible both in the ohmic and in the RF phases. They correspond to a sudden collapse of the temperature (see figure 5) in the central region ($2.8 \leqslant R \leqslant 3.65$ m in this case). The current interpretation (Wesson 1986) of this phenomena describes a catastrophic instability when the pitch angle of the line of force is such that the line of force closes exactly on itself after a rotation around the major axis ($m = 1$, $n = 1$ resonance). Similar oscillations but of smaller amplitude can also be seen on the central ion temperature.

The increase of central temperature measured in various experimental conditions appears well represented by the following law (figure 7)

$$(\Delta T_{e0} + \Delta T_{i0}) = aP_{RF}/\langle n_e \rangle,$$

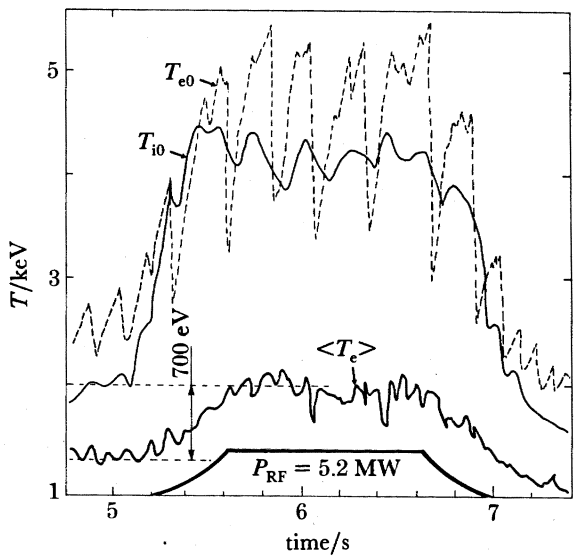

FIGURE 4. Evolution of the local (at $R = 3.15$ m) and volume-average temperatures resulting from a 5.2 MW pulse. The scatter is not due to measurement error but to large 'sawtooth'-like disruptions on the central electron temperature. Peak temperature occurs on the magnetic axis at 3.3 m, see figures 5 and 6. $I_p = 2$ MA, $B_\phi = 2.3$ T.

TABLE 2

	H minority $n_H/n_D = 5$–$10\,\%$	^{3}He $n_{^3He}/n_D = 5$–$10\,\%$
frequency	33 MHz	33 MHz
toroidal field (B_ϕ) on axis	2.3 T	3.4 T
plasma current (I_p)	2 MA	2, 3, 4 MA
average electron density	1.8×10^{19}–2.4×10^{19}	2×10^{19}–3.8×10^{19} m^{-3}
power coupled to the plasma	$\leqslant 5.5$ MW	$\lesssim 6$ MW
pulse duration	2 s	4 s

PHILOSOPHICAL TRANSACTIONS OF THE ROYAL SOCIETY A MATHEMATICAL, PHYSICAL & ENGINEERING SCIENCES

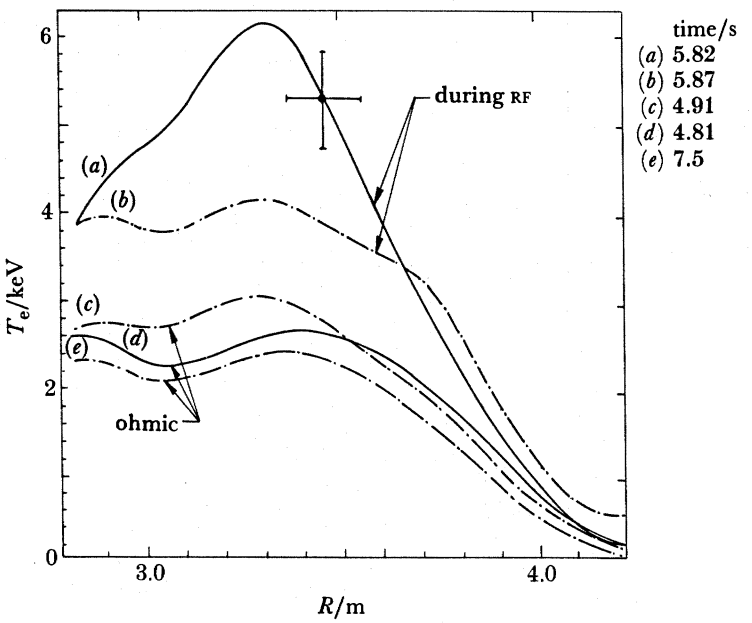

FIGURE 5. Electron-temperature profile before and during the heating pulse; the traces shown correspond to the top and to the bottom of a sawtooth.

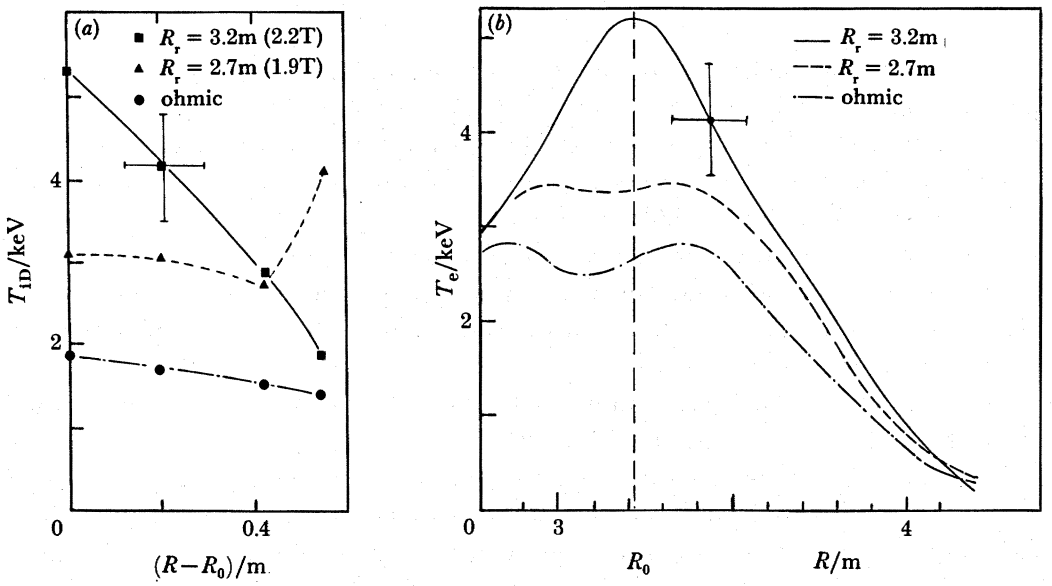

FIGURE 6. (*a*) Temperature profiles of the deuterons deduced from the neutral-particle analyser for central heating (R_r = 3.2 m) or off axis heating (R_r = 2.7 m). On the contrary, the electron temperature profile (*b*) remains unchanged outside the $q = 1$ surface.

where the central temperature increase has been time averaged on the sawteeth; a is only weakly dependent on I_p and B_ϕ taking a value of $(1.5–2) \times 10^{13}$ keV W^{-1} m^{-3} when I_p and B_ϕ are varied in the range

$$2.4 < B_\phi < 3.4, \quad 2 < I_p < 3 \text{ MA}.$$

The spatial distribution of the deuterium temperature as measured from the neutral-particle

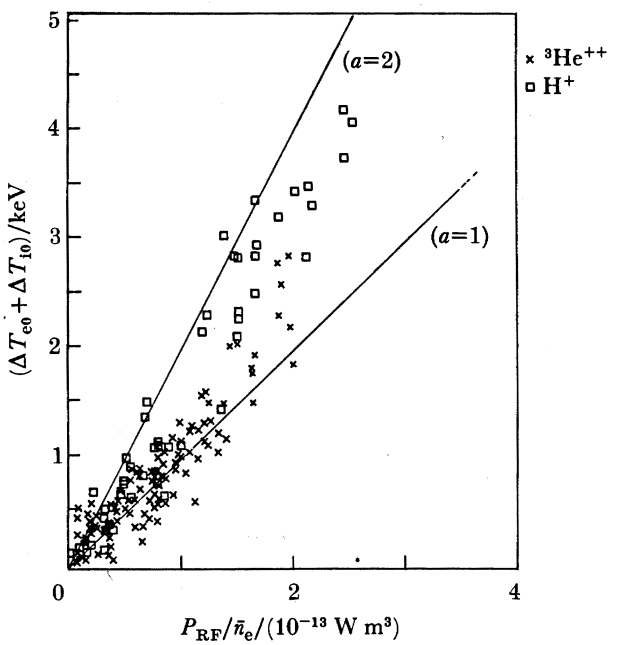

FIGURE 7. Central temperature increase $(\Delta T_{e0}+\Delta T_{i0})$ against RF power (normalized to mean density $\langle n_e \rangle$) for various discharges with $I_p = 2$ MA; $2.4\ \mathrm{T} < B_\phi < 3.4\ \mathrm{T}$; $1.2\times10^{19}\ \mathrm{m}^{-3} < \bar{n}_e < 2.5\times10^{19}\ \mathrm{m}^{-3}$ and $25\ \mathrm{MHz} < f < 33\ \mathrm{MHz}$.

analyser is illustrated in figure 6. Positioning the resonance near the plasma centre results in very peaked profiles similar to the electron-temperature profile (figure 5). Off-axis heating (figure 6) creates a flat ion-temperature profile. On the contrary, the electron temperature profile is not modified in the outer regions by off-axis heating. This phenomenon also observed in other tokamaks is known as 'profile consistency'.

The relative increase of the volume-average electron temperature $\langle T_e \rangle$ is always smaller than the relative increase of total input power and also smaller than the increase of the central electron temperature (figure 4). This is an indication that a degradation of confinement is localized in the outer part of the plasma.

This overview of heating effects is summarized in table 3. The other parameters for the same shot can be found in the first column of table 2.

The dominant effect, apart from the high temperature achieved, is that the stored energy W has only increased by a factor 2.5 despite an increase of the total input power by a factor of 4. This phenomenon is known as the degradation of energy confinement. It is often observed in tokamaks independently of the method used for additional heating. In this case the energy replacement time $\tau_E = W/P_{tot}$ drops from 0.48 ± 0.05 s to 0.3 ± 0.05 s. Note also that the ratio β_T (kinetic energy divided by the magnetic energy) is still modest and considerably lower than the limit set by ballooning modes (see Troyon, this symposium).

TABLE 3

	$10^{-19}n_{e0}$	P_Ω/MW	P_{tot}/MW	W/MJ	τ_E/s	$10^3\beta_T$
(before RF and after)	2.2	1.5	1.5	0.72	0.48	2
during RF	3	0.9	6.1	1.8	0.3	5

PHILOSOPHICAL TRANSACTIONS OF THE ROYAL SOCIETY A MATHEMATICAL, PHYSICAL & ENGINEERING SCIENCES

2.2. *Energy confinement times*

τ_E is the global energy confinement time: it describes the rate at which the energy has to be supplied to maintain stationary conditions. The pure ohmic heating conditions are characterized by τ_{Eo}. The evolution of τ_{Eo} with P_Ω (ohmic heating power) cannot be directly measured because P_Ω is not a free parameter being directly related to the plasma current. On the contrary, such information is available in additional heating experiments. The general observation is that the relation W against P_{tot} is linear to first order (figure 8). The lines do not intercept the origin and their vertical position mainly depends on the value of the plasma current. We may represent this global behaviour by the equation

$$W = \tau_{Eo} P_{\Omega o} + \tau_a (P_{tot} - P_{\Omega o}) = \tau_E P_{tot}.$$

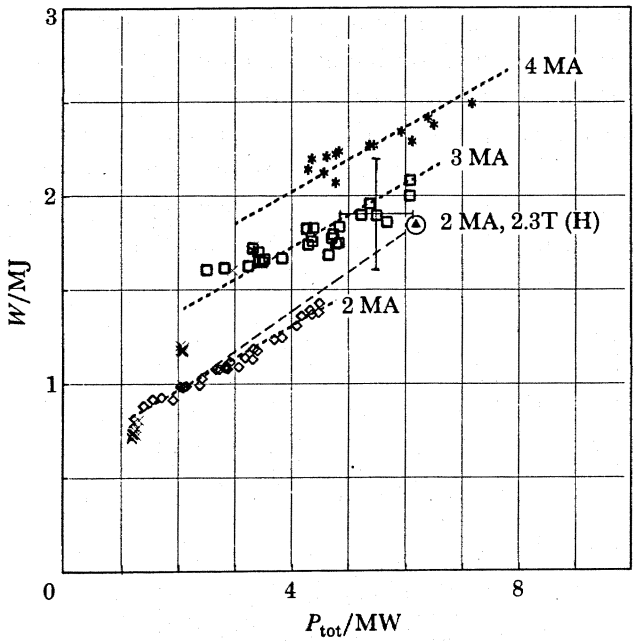

FIGURE 8. Stored energy against total power in a number of conditions. The toroidal field was normally 3.4 T and the minority ^{3}He except in one condition (H minority, 2.3 T).

Such a description suggests that as the power is increased the confinement goes through two phases (Rebut & Brusati 1986; Kadomtsev 1986). The first phase, at low input power as in most pure ohmic cases, is characterized by τ_{Eo}. τ_{Eo} obeys parametric dependence described by Gibson (this symposium). The second phase, characterized by τ_a, prevails at higher power or at higher density and corresponds to a reduced confinement $\tau_a \approx 0.3\,\tau_{Eo}$. τ_a is an important concept, which describes the confinement properties at the very large input power expected when additional heating is the dominant heat source. Such conditions will prevail with α-particle heating in ignited plasmas.

Our preliminary data base does not reveal a large dependence of τ_a with respect to P_{RF}, B_ϕ, I_p, n_e. It is interesting to note that a similar result using both NBI and RF was also obtained with a smaller tokamak (Odajima *et al.* 1987). τ_a is considerably larger than in smaller

tokamaks; a preliminary fit with data of Murakami *et al.* (1986), Steinmetz *et al.* (1986) and Odajima *et al.* (1986) in conditions similar to JET gives (figure 12)

$$\tau_a \approx 0.016\, aR^2 \sqrt{A_i},$$

where A_i is the atomic mass of the ions. This relation shows the great importance of the plasma size. Modes of operation with enhanced confinement times (roughly doubled) (Wagner 1982) have also been obtained in tokamaks that possess a divertor or a magnetic separatrix at the plasma boundary. Such operations are possible in JET, but have not yet been explored with additional heating.

2.3. *Effect of power localization*

As mentioned in the introduction, the ICRF power is deposited near the cyclotron resonance with a total width across the magnetic surfaces of about 30 cm (FWHM), which is sufficiently small compared to the plasma dimensions to allow the investigation of power localization on confinement. The localization is varied by changing the ratio of the toroidal field to the wave frequency. In the experiments analysed in figures 9–11, the wave frequency was fixed and magnetic field was varied from 2.6–1.9 T so that the cyclotron resonance was moved from 3.7–2.6 m. This range covers only the $q = 1$ volume. In this series of experiments, the increase of the plasma quantities due to a 4 MW RF pulse was measured by comparison to the same quantities at the same time without RF. It should be stressed that the variation observed may

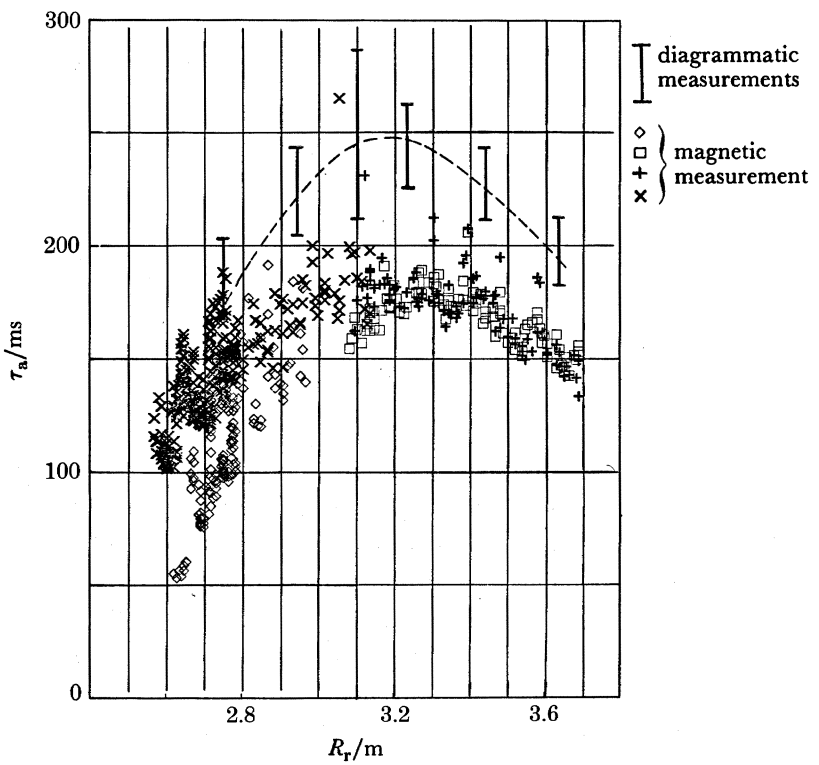

FIGURE 9. Asymptotic confinement time against position of the cyclotron resonance from two measurement techniques. The resonance position is varied by changing the magnetic field. The largest increase of stored energy is obtained when the resonance crosses the magnetic axis ($R_0 = 3.2$ m).

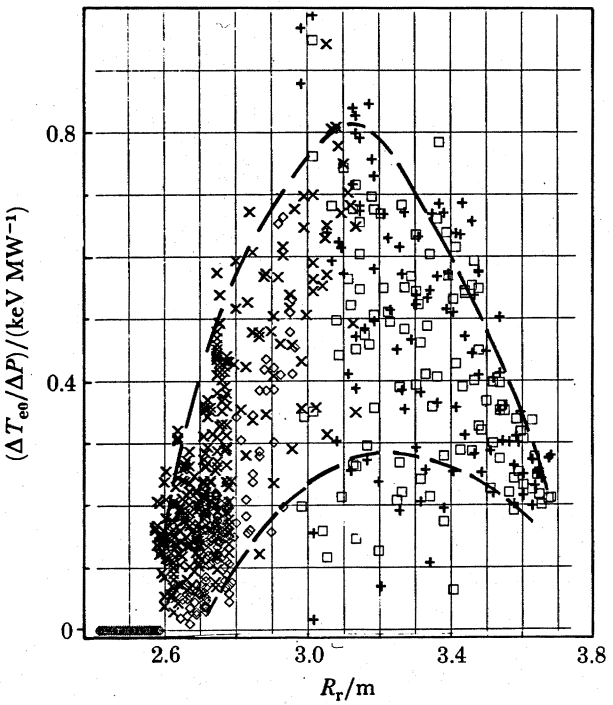

FIGURE 10. Electron-temperature increase, normalized to power increment, measured at 3.15 m, against the resonance position. The large scattering of the data results from the large sawteeth. Note that the sawteeth become small when the resonance is close to the $q = 1$ position (3.6 m).

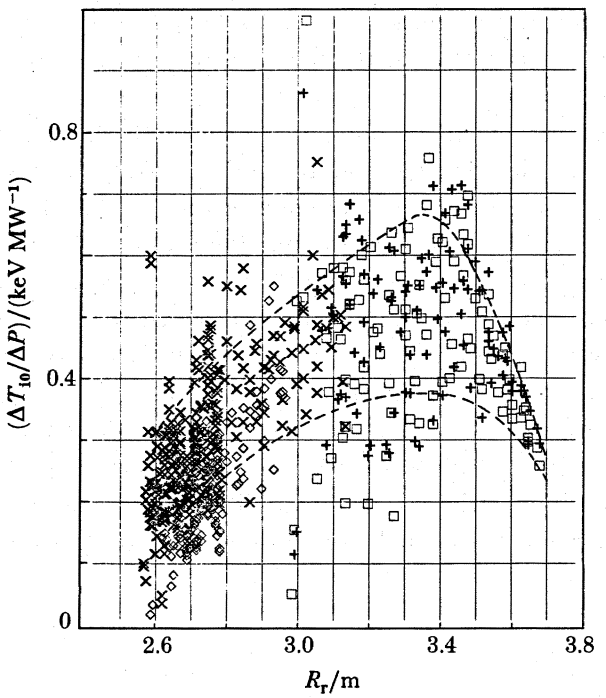

FIGURE 11. Central deuteron-temperature increase (neutron measurements) normalized to the power increment against the resonance position. The amplitude of the sawteeth as revealed by the data scattering is smaller in this case; note that the best heating condition corresponds to a resonance slightly displaced outboard.

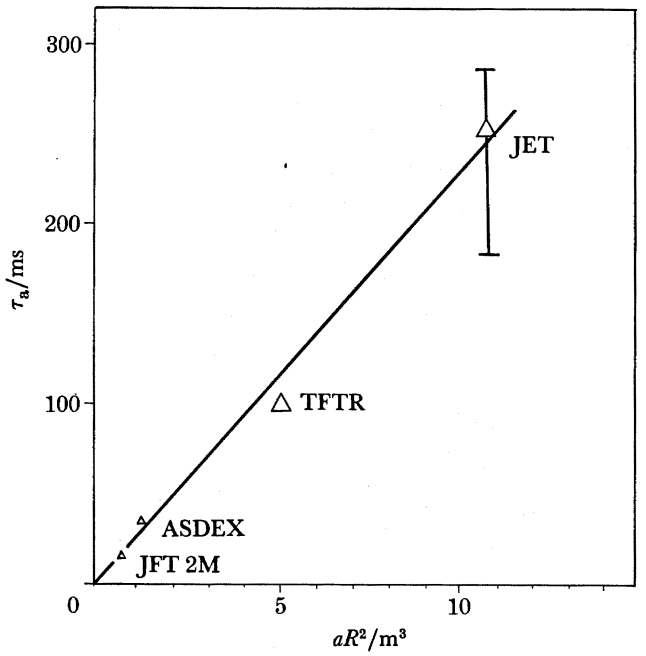

FIGURE 12. Asymptotic confinement times $\Delta W/\Delta P$ obtained in various experiments against aR^2 (a minor radius, R major radius).

be somewhat affected by the non-stationary plasma condition. Nevertheless, the following conclusions can be drawn.

(1) The largest values of τ_a are obtained with central heating. The exact value of τ_a obtained is uncertain as the various means of measurement do not agree exactly (figure 9). τ_a ranges between 180 and 250 ms.

The steep decrease observed when the resonance is on the high field side ($2.6 < R_r < 2.8$) may not be entirely due to a deteriorated confinement but to the increase of radiated power that is observed when the resonance is in this region or to a smaller damping of the waves.

(2) The largest central electron temperature increase is also observed when the resonance is located on the magnetic axis. This effect is illustrated on figure 10. The large scattering of the data in the figure is not due to poor signal:noise ratios but to the internal disruptions that are not synchronized with the sampling rate. The same figure also shows that the sawteeth are much reduced when the heating is outside the $q = 1$ surface.

(3) The largest increase of central ion temperature is observed when the resonance is slightly displaced outwards by *ca.* 20 cm (figure 11). Again the scattering of the data points on this figure is due to the sawtoothing activity but the amplitude of the ion temperature fluctuation is smaller than on the electron temperature. Comparable average electron and ion temperature increases are observed.

3. Conclusions

(i) The method of plasma heating with ion-cyclotron resonance at megawatt power level appears well founded. As expected, the power is locally deposited and transferred via the resonant minority ion species to plasma electrons and ions with roughly an equal share.

(ii) For a 3 MA plasma, central temperatures, time-averaged over the sawteeth have reached 4 keV for both the electrons and the ions at a central density n_{e0} of 4.5×10^{19} cm^{-3} ($\langle n_e \rangle = 3 \times 10^{19}$ m^{-3}). Higher temperatures can be reached at lower density following a law $(\Delta T_{e0} + \Delta T_{i0}) = aP_{RF}/\langle n_e \rangle$, with $a = (1.5\text{–}2)\ 10^{13}$ keV W^{-1} m^3.

(iii) The effect of degradation of energy confinement with increased input power is similar to the results obtained with smaller tokamaks. However, the confinement times are considerably larger in JET in qualitative agreement with a law depending on the cube of the dimensions (figure 12).

References

Adam, J. & Samain, A. 1971 Report no. EUR-CEA-FC 579. CEN, Fontenay-aux-Roses.

Bhatnagar, V. P. *et al.* 1983 In *Proc. 9th International Conference on Plasma Physics and Controlled Nuclear Fusion Research, Baltimore, 1–8 September 1982*, vol 2, p. 103. Vienna: IAEA.

Équipe TFR 1977 In *Proc. 6th International Conference on Plasma Physics and Controlled Nuclear Fusion Research, Berchtesgaden, 6–13 October 1987*, vol. 1, p. 69. Vienna: IAEA.

Hellsten, T. *et al.* 1985 *Nucl. Fusion* **25**, 99.

Hooke, W. M., Avivi, P., Brennan, M. H., Rothman, M. A. & Stix, T. H. 1962 Experiments on ion cyclotron waves. *Nucl. Fusion Suppl.* part 3, 1083.

Itoh, S., Itoh, K. & Fukuyama, A. 1986 JET-R (86) 02.

Jacquinot, J. *et al.* 1985 *Plasma Phys. controlled Fusion* **27**, 1379.

Jacquinot, J. *et al.* 1986 *Plasma Phys. controlled Fusion* **28**, 1.

Kadomtsev, B. B. 1986 *Plasma Phys. controlled Fusion* **28**, 125.

Kaye, A. S. *et al.* 1985 In *Proc. 11th Symposium on Fusion Engineering, Austin, Texas, 18–22 November 1985*, cat no. CH 2251–7. New York: IEEE.

Murakami, M. *et al.* 1986 *Plasma Phys. controlled Fusion* **28**, 17.

Odajima, K. *et al.* 1987 Confinement Studies During ICRF Experiments in JFT2M, JAERI report (In the press.).

Pease, R. S., Yoshihawa, S. & Eubank, P. 1966 The confinement of plasma heated by ion cyclotron resonance in the C stellarator. Preprint no. MATT-87, University of Princeton, New Jersey.

Rebut, P. H. & Brusati, M. 1986 *Plasma Phys. controlled Fusion* **28**, 113.

Steinmetz, K. *et al.* 1986 *Plasma Phys. controlled Fusion* **28**, 235.

Wagner, F. *et al.* 1982 *Phys. Rev. Lett.* **49**, 1408.

Wesson, J. A. 1986 *Plasma Phys. controlled Fusion* **28**, 243.

PHILOSOPHICAL TRANSACTIONS OF THE ROYAL SOCIETY A MATHEMATICAL, PHYSICAL & ENGINEERING SCIENCES